Neuron, Vol. 46, 191–204, April 21, 2005, Copyright ©2005 by Elsevier Inc. DOI 10.1016/j.neuron.2005.01.030

Eph-Dependent Tyrosine Phosphorylation of Ephexin1 Modulates Growth Cone Collapse

Mustafa Sahin,[1,2,7] Paul L. Greer,[1,7] Michael Z. Lin,[1,7] Heather Poucher,[3] Johann Eberhart,[4] Susanne Schmidt,[5] Tracy M. Wright,[1] Steven M. Shamah,[1] Sinead O'Connell,[4] Christopher W. Cowan,[1] Linda Hu,[1] Jeffrey L. Goldberg,[6] Anne Debant,[5] Gabriel Corfas,[1] Catherine E. Krull,[3] and Michael E. Greenberg[1,*]

[1]Neurobiology Program
Children's Hospital and
Departments of Neurology and Neurobiology
Harvard Medical School
Boston, Massachusetts 02115
[2]Department of Neurology
Children's Hospital
Boston, Massachusetts 02115
[3]Cell and Developmental Biology
University of Michigan
Ann Arbor, Michigan 48109
[4]Biological Sciences
University of Missouri-Columbia
Columbia, Missouri 65211
[5]Centre de Recherches en Biochimie
Macromoléculaire
FRE 2593
Centre National de la Recherche Scientifique
1919 Route de Mende
34293 Cedex 5 Montpellier
France
[6]Bascom Palmer Eye Institute
University of Miami
Miami, Florida 33136

Summary

Ephs regulate growth cone repulsion, a process controlled by the actin cytoskeleton. The guanine nucleotide exchange factor (GEF) ephexin1 interacts with EphA4 and has been suggested to mediate the effect of EphA on the activity of Rho GTPases, key regulators of the cytoskeleton and axon guidance. Using cultured *ephexin1*$^{-/-}$ mouse neurons and RNA interference in the chick, we report that ephexin1 is required for normal axon outgrowth and ephrin-dependent axon repulsion. Ephexin1 becomes tyrosine phosphorylated in response to EphA signaling in neurons, and this phosphorylation event is required for growth cone collapse. Tyrosine phosphorylation of ephexin1 enhances ephexin1's GEF activity toward RhoA while not altering its activity toward Rac1 or Cdc42, thus changing the balance of GTPase activities. These findings reveal that ephexin1 plays a role in axon guidance and is regulated by a switch mechanism that is specifically tailored to control Eph-mediated growth cone collapse.

*Correspondence: michael.greenberg@childrens.harvard.edu
[7]These authors contributed equally to this work.

Introduction

The establishment of precisely wired neuronal networks between the approximately 10^{11} neurons in the central nervous system (CNS) presents a tremendous challenge for mammalian development. During ontogeny, newly generated neurons must migrate to their appropriate location within the brain. As they reach their final destination, these cells extend axons and form synapses onto their targets to generate appropriate neuronal circuits. Each of these steps depends on the ability of neurons to respond to a complex set of environmental cues and modify their intrinsic maturation program. Over the last decade, significant progress has been made in identifying both the extracellular factors and neuronal receptors that regulate neuronal development. Such factors include secreted molecules such as semaphorins, slits, and netrins, as well as membrane-associated molecules such as ephrins (Dickson, 2002; Huber et al., 2003). Neurons and their growth cones respond to these guidance factors through the coordinated regulation of a variety of intracellular processes including endocytosis, protein and lipid transport, actin cytoskeletal remodeling, the modulation of microtubule dynamics, and protein synthesis and degradation. A key, unresolved issue is how cell surface receptors promote these diverse cellular processes to elicit specific cellular responses such as neuronal migration, growth cone guidance, and synapse formation.

To begin to address this question, we investigated the signaling mechanisms by which the Eph family of receptor tyrosine kinases mediates cellular responses. With 13 members in the mouse and human genomes, Ephs can be divided into two subfamilies (EphA and EphB) that together constitute the largest known family of receptor tyrosine kinases. The Ephs and their ligands, the ephrins, are broadly expressed throughout the developing nervous system (Flanagan and Vanderhaeghen, 1998; Palmer and Klein, 2003). Eph signaling contributes to a wide variety of developmental processes including early patterning events responsible for hindbrain segmentation as well as the migration of neural crest cells during development. The best-characterized role of Eph signaling involves the guidance of axons during neural development. Gene knockout experiments have demonstrated a role for ephrin-Eph signaling in the pathfinding of axons, including axons of the corticospinal tract, the corpus callosum, and the anterior commissure, as well as retinotectal map formation, motor axon projections to the periphery, and thalamocortical projections (Palmer and Klein, 2003).

Ephs likely mediate aspects of neural development by controlling cytoskeletal function through regulation of the Rho family GTPases, RhoA, Rac1, and Cdc42 (Penzes et al., 2003; Wahl et al., 2000; Winning et al., 2002). These small, monomeric GTPases function as molecular switches, cycling between an inactive GDP bound state and an active GTP bound form in which they activate downstream effectors (Van Aelst and D'Souza-Schorey, 1997). Each of the Rho family mem-

bers promotes the formation of distinct actin structures in cells. For example, in neuronal growth cones, activated RhoA causes growth cone repulsion by enhancing actin cytoskeleton contractility, while Rac1 and Cdc42 promote extension by inducing the formation of actin-based lamellipodia and filopodia, respectively.

Rho GTPase activation is controlled by the opposing actions of guanine nucleotide exchange factors (GEFs), which catalyze the exchange of GDP for GTP, and GTPase activating proteins (GAPs), which promote hydrolysis of GTP to GDP. Recently, we identified a Dbl family GEF, termed ephexin1, which interacts with the cytoplasmic domain of EphA4 (Shamah et al., 2001). Ephexin1 is highly expressed in the CNS during development and is enriched in neuronal growth cones. When overexpressed in cells, ephexin1 activates RhoA, Rac1, and Cdc42. The coexpression of activated EphA4 with ephexin1 enhances the ability of ephexin1 to activate RhoA relative to its ability to activate Rac1 and Cdc42, thereby promoting growth cone collapse. However, the relative importance for axon guidance of ephexin1 compared to other GEFs and the mechanism by which EphA signaling regulates ephexin1 activity remained to be determined.

In this study, we find that, in the absence of ephrin stimulation, ephexin1 promotes axon growth. We also demonstrate that ephexin1 is required for ephrin-A-induced growth cone collapse of retinal ganglion cells (RGC) and the Eph/ephrin-mediated stalling of spinal motor axons at the base of the limb in vivo. Thus, ephexin1 is involved in the opposing processes of axonal outgrowth and growth cone collapse/repulsion. We have elucidated the mechanism by which Ephs control ephexin1's activity to mediate these processes. We find that, in the absence of ephrin stimulation, ephexin1 activates RhoA, Rac1, and Cdc42, thus leading to a balance of GTPase activity that promotes outgrowth. Ephrin engagement of Ephs leads to phosphorylation of ephexin1 on Tyr87. This phosphorylation event preferentially activates ephexin1's exchange activity toward RhoA but not Rac1 and Cdc42, thus switching the substrate preference of ephexin1 and leading to growth cone collapse. These findings reveal a new mode of phosphorylation-dependent GEF regulation and provide insight into the mechanism by which EphA signaling controls the actin cytoskeleton via ephexin1 phosphorylation.

Results

Ephexin1-Deficient RGCs Have a Deficit in Ephrin-A-Induced Growth Cone Collapse

We have previously shown that EphA4 and ephexin1 interact when expressed in HEK293T cells (Shamah et al., 2001). In addition, overexpression of a dominant interfering form of ephexin1 in RGCs leads to an inhibition of ephrin-induced growth cone collapse. Nonetheless, we have been unable to detect an interaction between endogenous EphAs and ephexin1 in neurons by coimmunoprecipitation, leaving open the possibility that, when overexpressed in neurons, inactive ephexin1 occludes the binding of a GEF other than ephexin1 that under physiological conditions is the actual mediator of ephrin-A-induced growth cone collapse. To address the question of whether ephexin1 mediates ephrin-A-induced growth cone collapse under physiological conditions, we generated mice in which the *ephexin1* gene is disrupted and asked whether, in *ephexin1*$^{-/-}$ neurons, ephrin-A is still effective at inducing RGC growth cone collapse.

ephexin1$^{-/-}$ mice were generated by standard methods (Figure S1A), were born at the expected Mendelian frequency, and were viable, fertile, and overtly normal, possibly due to the presence of other members of the ephexin family (see below). Western blot analyses of whole brain lysates with any of four distinct antibodies raised against either the N- or C-terminal domains of ephexin1 failed to detect the presence of ephexin1 protein in *ephexin1*$^{-/-}$ mice (Figure 1A; Figure S1B). Furthermore, immunohistochemistry of wild-type and *ephexin1*$^{-/-}$ brain sections revealed strong, specific immunoreactivity in the striatum and neocortex of wild-type mice and no immunoreactivity in the brains of *ephexin1*$^{-/-}$ mice (Figure 1B).

As ephexin1 has previously been shown to activate RhoA, Rac1, and Cdc42 (Shamah et al., 2001) and these GTPases are known to be involved in axon extension, we investigated whether *ephexin1*$^{-/-}$ RGCs have defects in axon extension. We measured the length of the axon in RGC cultures from wild-type and *ephexin1*$^{-/-}$ mice. Axons from *ephexin1*$^{-/-}$ RGCs were significantly shorter than their counterparts from wild-type RGCs (Figure 2A; wild-type 151.9 ± 13.8 μm versus *ephexin1*$^{-/-}$ 110.7 ± 8.4 μm; $p < 0.01$ by ANOVA). However, the number of neurites per cell was unaltered between wild-type and *ephexin1*$^{-/-}$ neurons (wild-type 3.87 ± 0.22 versus *ephexin1*$^{-/-}$ 4.19 ± 0.11 neurites per cell; $p = 0.32$ by ANOVA). These results suggest that ephexin1 plays a crucial role in axon outgrowth.

Our previous study had suggested that ephexin1 might play a role in regulating ephrin-induced growth cone collapse in RGCs. To assess the importance of ephexin1 for EphA-mediated axon guidance, we compared the ability of ephrin-A to induce growth cone collapse of RGCs obtained from either wild-type or *ephexin1*$^{-/-}$ mice. We used purified RGCs for these experiments, because both EphAs and ephexin1 are expressed in the ganglion cell layer of embryonic and early postnatal retina, and the ability of ephrins to mediate growth cone collapse has been well established in RGCs (Feldheim et al., 1998; Jurney et al., 2002; Shamah et al., 2001). Purified RGCs from wild-type and *ephexin1*$^{-/-}$ mice have a similar percentage of intact growth cones prior to ephrin treatment (Figure 2B). Upon exposure to ephrin-A1, RGCs from wild-type mice show a significant increase in the number of collapsed growth cones. By contrast, significantly fewer *ephexin1*$^{-/-}$ RGC growth cones collapse in response to ephrin-A1 (Figure 2B; percent uncollapsed mean ± SEM with ANOVA: wild-type, 30.4 ± 1.4; *ephexin1*$^{-/-}$, 53.3 ± 3.2; $p < 0.01$). This reduction in the percentage of collapsed growth cones in *ephexin1*$^{-/-}$ versus wild-type neurons does not reflect an intrinsic defect in the ability of RGCs to respond to repulsive factors; when RGCs from wild-type and *ephexin1*$^{-/-}$ mice were exposed to lysophosphatidic acid (LPA), an agent that induces growth cone collapse via a G protein-coupled receptor that triggers RhoA activation (Moolenaar, 1999), we de-

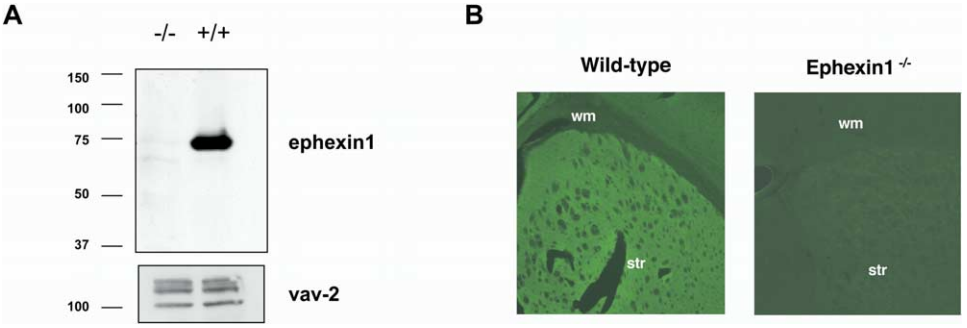

Figure 1. Characterization of *ephexin1*$^{-/-}$ Mice

(A) Western blot demonstrating the absence of ephexin1 protein in *ephexin1*$^{-/-}$ mice. Vav-2, another Rho family GEF, serves as a loading control.

(B) Immunohistochemistry of brain sections from wild-type and *ephexin1*$^{-/-}$ mice revealed specific staining in the striatum (str) and neocortex of wild-type mice above the white matter (wm). There is no detectable staining in brain sections from *ephexin1*$^{-/-}$ mice.

tected no significant difference in growth cone collapse between wild-type and *ephexin1*$^{-/-}$ RGCs (Figure 2B). Furthermore, levels of both phosphorylated and non-phosphorylated Ephs were unaltered in *ephexin1*$^{-/-}$ RGCs when compared to wild-type RGCs (data not shown). These results suggest that, although the basic cellular machinery that mediates growth cone formation and collapse is intact in ephexin1-deficient neurons, EphA-mediated growth cone collapse is impaired in the absence of ephexin1.

Since cultured RGCs from *ephexin1*$^{-/-}$ mice have defects in axonal outgrowth as well as in ephrin-induced growth cone collapse, we asked whether these phenotypes would be recapitulated in vivo in *ephexin1*$^{-/-}$ mice. However, by axon tracing experiments, we have been unable to detect a defect in axon pathfinding in *ephexin1*$^{-/-}$ retinogeniculate, retinocollicular, or corticospinal tracts (data not shown). We suspected that the absence of overt axonal phenotype in *ephexin1*$^{-/-}$ animals might be a result of compensation by other ephexin family members. In our earlier study, we identified three human homologs of ephexin1 (Shamah et al., 2001). Taking advantage of the recent publication of the human genome sequences, we have now identified an additional human ephexin family member (RET/ARHGEF19). Using the BLAST program to search the EST and genomic databases, we also identified four mouse genes that are highly homologous to the original mouse *ephexin1*. We named these human and mouse genes *ephexin2* through *ephexin5* based on their sequence similarity to the original *ephexin* gene (Figure 2C). We now refer to the original isolate as ephexin1

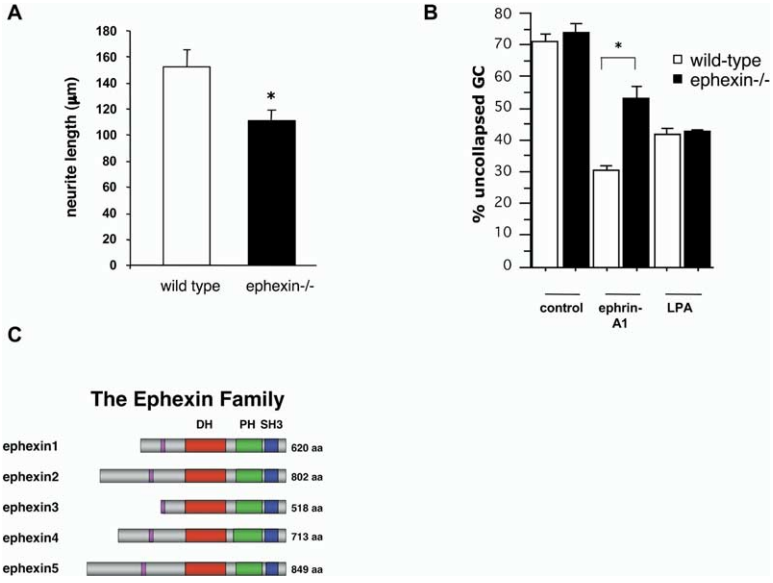

Figure 2. Ephexin1 Is Required for Ephrin-Induced Growth Cone Collapse

(A) *ephexin1*$^{-/-}$ RGCs have shorter neurites compared to RGCs from wild-type littermates. These data represent four separate experiments in which at least 50 neurites were measured for each condition. All experiments were scored in a blinded manner. All error bars are standard error of the mean (SEM); *$p < 0.01$.

(B) *ephexin1*$^{-/-}$ RGCs collapse less efficiently in response to ephrin stimulation. However, there is no difference between wild-type and knockout cells in the percentage of collapsed growth cones following LPA treatment. These data represent three separate experiments in which at least 100 growth cones were scored for each condition. All experiments were scored in a blinded manner. All error bars are SEM; *$p < 0.01$.

(C) Schematic representation of the five murine ephexin family members. The SH3 domain is indicated in blue, the PH domain is indicated in green, the DH domain is indicated in red, and the conserved tyrosine motif at the N terminus is indicated in purple. The numbers on the right indicate the number of amino acids contained in each full-length ephexin family member.

and use the term ephexin family to refer to this group of five mammalian genes. A comparison of the sequence of the five ephexin family members reveals that they share the same overall structure, including a Dbl homology (DH) domain followed by a pleckstrin homology (PH) domain, and a C-terminal SH3 domain. However, the various members of the ephexin family have unique N-terminal regions, which are variable in length and have little sequence similarity. Examination of the tissue distribution of the ephexin family members by Northern blot and in situ hybridization revealed that only ephexin1 and ephexin5 (also known as Vsm-RhoGEF [Ogita et al., 2003]) mRNA are detected at significant levels in P7 and P21 mouse brain (Figure S2).

Ephexin Is Expressed Differentially in Chick Motor Neuron Columns

Since our analysis of *ephexin1*$^{-/-}$ mice appears to be complicated by issues of compensation by other ephexin family members, we searched for an organism with only one ephexin ortholog. We chose the chick embryo because only a single ephexin is expressed, and EphA4 and ephrins play important roles in the guidance and patterning of motor axons to their targets (Eberhart et al., 2002; Eberhart et al., 2004). At hindlimb levels, motor neurons are organized into lateral and medial motor columns [LMC and MMC(m)], respectively. While both subsets of neurons express EphA4, LMC and MMC(m) neurons respond differentially to ephrin-A5 (Eberhart et al., 2004). Axons of motor neurons in the lateral portion of the LMC are repelled by ephrin-A5 in limb mesoderm, whereas MMC(m) axons extend readily into ephrin-A5-expressing somitic mesoderm. We considered the possibility that the differential response of LMC and MMC(m) axons to ephrin-A might reflect differences in the ability of EphA4 to signal to ephexin.

To determine if ephexin protein is differentially expressed in LMC and MMC(m) neurons, we examined its distribution using an anti-chicken ephexin antibody. Endogenous chicken ephexin (c-ephexin) localizes to LMC neurons but is absent from MMC(m) neurons (Figure 3A). This observation raised the possibility that c-ephexin may account for the differential responses of these motor axons to ephrins. MMC(m) neurons may extend axons readily into the ephrin-A5-positive somitic mesoderm because they lack c-ephexin, while LMC axons that express c-ephexin might be prohibited from entering the ephrin-expressing limb mesoderm. If LMC axons utilize c-ephexin in their inhibitory response, then one would predict that the loss of c-ephexin would result in the premature entry of LMC axons into the limb mesoderm.

Motor Axons Sort and Enter the Limb Prematurely When c-Ephexin Levels Are Reduced

To test whether c-ephexin plays a role in the LMC axon pathfinding, we generated two shRNA constructs directed against c-ephexin, transfected them into chick neural tubes, and examined their effect on motor neuron projections. We first tested the ability of these shRNA constructs to knock down c-ephexin in HEK293T cells and found that they significantly reduced c-ephexin protein levels compared to control constructs (Figure 3B), indicating that our shRNA constructs reduce c-ephexin protein levels in vitro. To determine whether c-ephexin is required for LMC axons to stall at the base of the limb, the right side of neural tubes from stage 17 embryos was transfected with either of two c-ephexin shRNA constructs and an EGFP plasmid. To ascertain whether c-ephexin protein was reduced in transfected neurons, transverse sections through embryos were stained with anti-c-ephexin antibody and Islet-1/2 antibody, to mark postmitotic motor neurons, followed by quantification of pixel intensity. C-ephexin protein levels are reduced in neurons transfected with c-ephexin shRNA/EGFP, compared with control conditions (Figure 3C). Motor neurons were generated in their appropriate position and number; EphA4 protein levels were unaltered in neurons transfected with c-ephexin shRNA (data not shown). These results demonstrate that shRNA against c-ephexin reduces c-ephexin protein specifically in LMC neurons in vivo.

We next examined the effects of knocking down c-ephexin on the projections of LMC neurons. When c-ephexin levels are reduced, motor axons extend prematurely into the limb mesoderm (n = 6 embryos; Figures 3D and 3E). In addition, EphA4 protein becomes segregated early to a subset of motor axons, localizing to the forming dorsal nerve trunk (Figures 3D and 3E). Three sets of controls were examined: (1) motor axons expressing EGFP alone (n = 5 embryos); (2) motor axons transfected with missense shRNA constructs against c-ephexin (n = 5 embryos); and (3) nontransfected, contralateral motor axons (n = 12 embryos). In all three controls, motor axons remained at the base of the limb and did not enter limb mesoderm early (Figures 3D and 3E). These results indicate that c-ephexin is required in LMC axons in vivo to elicit their stalling behavior at the base of the hindlimb mesoderm. Having demonstrated that ephexin is required for Eph signaling in vivo, we sought to understand the mechanism by which Ephs signal to ephexin to regulate the actin cytoskeleton.

Eph Kinase Activity Is Required for Regulating Ephexin1

We found that treating cultured RGCs with clustered ephrin-A1 leads to growth cone collapse and that to occur normally this process requires ephexin1. Since treatment with clustered ephrins induces the aggregation of Ephs, leading to the induction of EphA tyrosine kinase activity, it was possible that either the aggregation of EphA or the induction of EphA kinase activity was responsible for ephexin1 activation. To determine if the tyrosine kinase activity of Ephs is required for ephexin1 activation, we introduced EphA4 and ephexin1 into fibroblasts and monitored the ability of EphA4 to regulate ephexin1-dependent RhoA, Rac1, and Cdc42 activation. Fibroblasts provide a facile system for evaluating the effects of EphA and ephexin1 on RhoA, Rac1, and Cdc42 activity, as activation of these Rho family GTPases triggers specific changes in fibroblast morphology that can be visualized by phalloidin staining. In fibroblasts, RhoA induces stress fiber formation, Cdc42 causes filopodia extension, and Rac1 triggers lamellipodia formation and membrane ruffling (Nobes

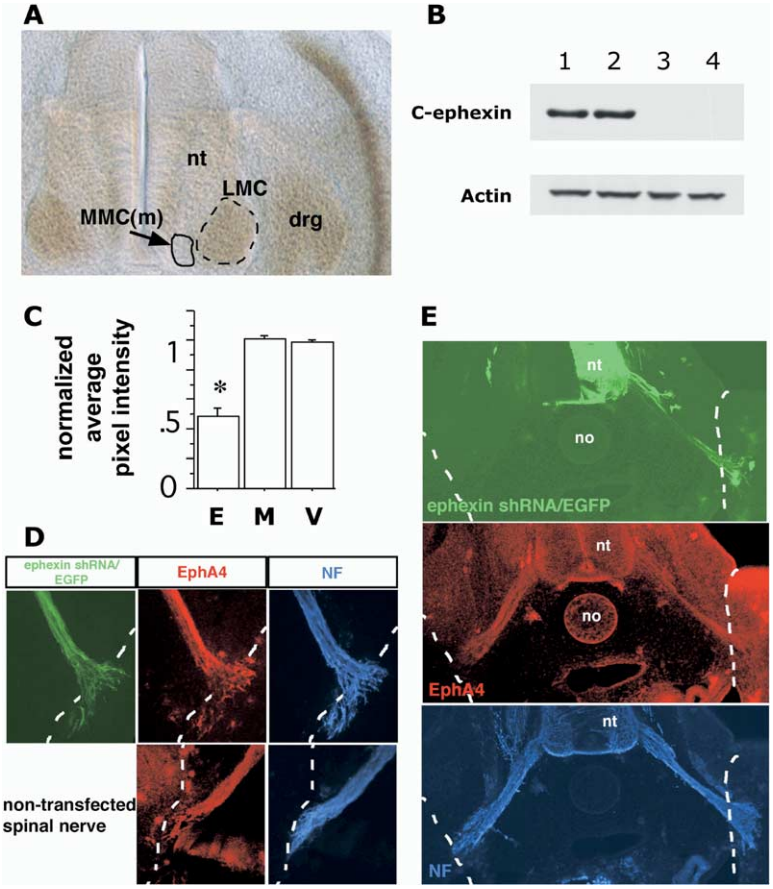

Figure 3. Chick Motor Neuron Axons Sort and Enter the Hindlimb Prematurely When Ephexin Is Knocked Down

(A) Expression of chick ephexin in the neural tube (nt) using an anti-chick ephexin antibody. Labeling localizes to motor neurons in the lateral motor column (LMC) but not the medial motor column [MMC(m)]. C-ephexin protein is also present in the forming dorsal root ganglia (DRG) and the myotome.

(B) shRNAs directed against c-ephexin reduce c-ephexin protein levels in HEK293T cells. Cells were transfected with c-ephexin (lane 1), c-ephexin and shRNA vector (lane 2), c-ephexin and shRNA 461 (lane 3), or c-ephexin and shRNA 218 (lane 4). Lysates were probed with antibodies against c-ephexin and actin, which serves as a loading control.

(C) shRNA directed against c-ephexin reduces c-ephexin protein levels in chick neural tubes. Average pixel intensity following immunohistochemistry with anti-c-ephexin antibody for stage 23 presumptive LMC motor neurons was calculated for transfected and untransfected sides of chick embryos. shRNA directed against chick ephexin ("E"; n = 5), missense shRNA ("M"; n = 4), and EGFP-expressing vector ("V"; n = 2) were compared for ephexin expression. The y axis denotes the ratio of average pixel intensity between transfected and untransfected sides. shRNAs directed against chicken ephexin specifically reduce ephexin protein levels. All error bars are SEM; *$p < 0.0001$.

(D) Top: Motor axons that express ephexin shRNAs sort and project into the hindlimb prematurely. White dashed line demarcates the base of the limb, which was determined by the expression of EphA4 in limb mesoderm. (Left) Motor axons treated with ephexin shRNAs express EGFP (green); (middle) EphA4 protein (red) decorates the forming dorsal nerve trunk; (right) neurofilament antibody labeling (blue) marks all motor axons. Bottom: Nontransfected motor axons stall at the base of the limb. EphA4 protein (middle; red) and neurofilament antibody (right; blue) mark all motor axons in the spinal nerve.

(E) Three optical sections acquired from the same embryo, treated with ephexin shRNAs on the right neural tube (nt). Left neural tube is not transfected. White dashed line indicates base of hindlimb; no, notochord. Top: EGFP expression (green) localizes to most cells in the ventral neural tube and several motor axons that have projected to the limb. Middle: EphA4 protein (red) becomes segregated to a subset of axons (arrow), in the presence of ephexin shRNAs. Note that all motor axons on the nontransfected side express EphA4. Bottom: Neurofilament antibody (blue) labels ephexin shRNA-transfected and nontransfected motor axons.

and Hall, 1995). We have previously shown that, when expressed in REF-52 fibroblasts, ephexin1 induces morphologic changes consistent with the activation of the GTPases RhoA, Cdc42, and Rac1 (Shamah et al., 2001; Figure 4A). However, when EphA4 is coexpressed with ephexin1 in REF-52 cells, there is an increase in the percentage of cells displaying stress fibers (RhoA phenotype) and a decrease in the percentage of cells with lamellipodia and filopodia (Rac1 and Cdc42 phenotypes, respectively). These results suggest that EphA4 enhances the ability of ephexin1 to activate RhoA and/or inhibits ephexin1 activation of Rac1 and Cdc42, thus resulting in a shift in the balance of Rho GTPase activities.

To test whether the kinase activity of EphA4 is required for this shift in GEF activity, we generated a point mutation in EphA4, which renders it kinase inactive. In contrast to wild-type EphA4, expression of the kinase-inactive EphA4 did not affect the percentage of ephexin1-expressing cells exhibiting RhoA, Rac1, and Cdc42 phenotypes (Figure 4A). These findings indicate that the kinase activity of EphA4 is necessary for the ability of EphA to modulate ephexin1 GEF activity. As cells expressing equal levels of wild-type or kinase-inactive EphA4 showed no obvious differences in the level of ephexin1 expression, ephexin1 subcellular localization, or ephexin1 association with EphA4 (data not shown), we focused our attention on the possibility that, upon activation, EphA4 might lead to the phosphorylation of ephexin1 and thereby might modulate ephexin1 function.

Ephexin Family Members Contain a Conserved Phosphorylation Site

Reasoning that sites of phosphorylation that play an important role in regulating ephexin1 function would be conserved throughout evolution, we identified tyrosine residues within the ephexin family that are conserved and might therefore represent regulatory phosphorylation sites. By comparing the sequences of the five mammalian ephexins and the chicken, *Drosophila*, and *C. elegans* ephexin orthologs, we identified a single ty-

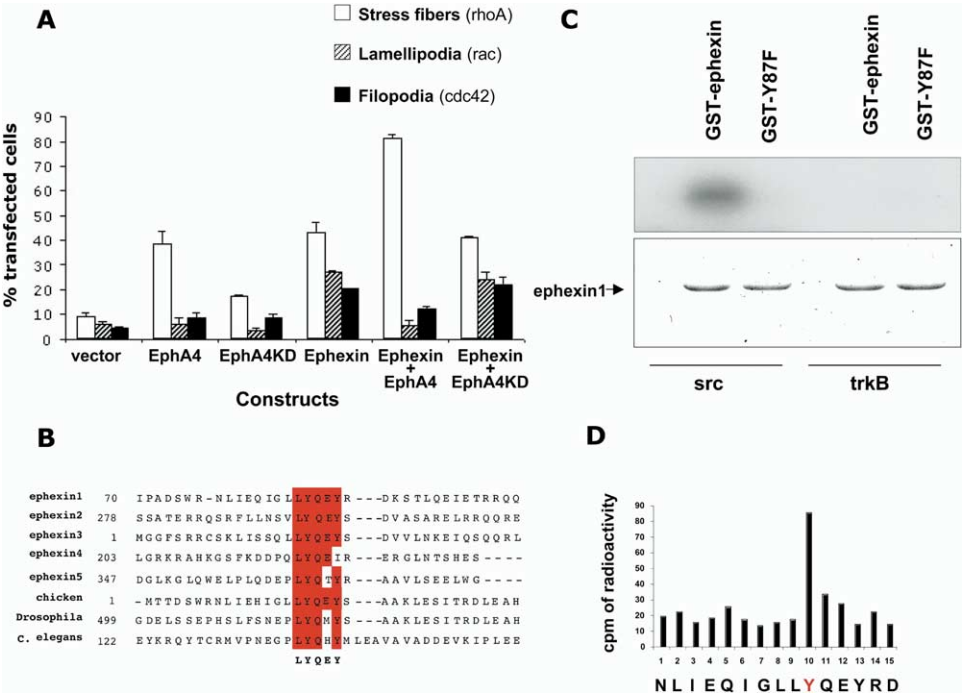

Figure 4. Phosphorylation of a Conserved N-Terminal Tyrosine Residue of Ephexin1

(A) REF-52 cells transfected with wild-type or kinase-dead EphA4 and ephexin1. Cells were stained with fluorescent phalloidin and scored in a blinded manner for the presence of stress fibers (white bars), lamellipodia (hatched bars), and filopodia (black bars). All transfections were repeated three times, and at least 120 cells were scored in a blinded manner for each condition. All error bars are SEM.

(B) Sequence alignment of the *Mus musculus*, *Gallus gallus*, *Drosophila melanogaster*, and *Caenorhabditis elegans* ephexin family members reveals a conserved N-terminal motif (highlighted in red). The first tyrosine in this motif is conserved in all family members.

(C) In vitro kinase assays with Src and trkB. Wild-type ephexin1 or ephexin1-Y87F were used as substrates for the kinases. Samples were electrophoresed on an SDS-PAGE gel, which was subsequently stained with Coomassie blue to demonstrate equal loading and exposed to film. Autoradiograph (top); Coomassie staining (bottom).

(D) Verification that Tyr87 is phosphorylated in ephexin1. Ephexin1 that was phosphorylated in vitro was subjected to tryptic digestion and Edman degradation. Graph represents scintillation count associated with each amino acid as it was released by Edman degradation.

rosine corresponding to amino acid 87 (Tyr87) of ephexin1 that is present in the unique N-terminal region of ephexin1 and is conserved between all ephexin family members (Figure 4B). Analysis using the Scansite phosphorylation prediction program revealed that Tyr87 lies within a stretch of amino acids that form a consensus site for Src family kinase phosphorylation (http://scansite.mit.edu/). As EphA4 is similar to Src in its substrate preference, we considered the possibility that ephexin1 Tyr87 is a site of phosphorylation by the Eph kinase and/or a Src family member.

To test if Tyr87 can be phosphorylated by Src or EphA4, we incubated recombinant Src or the EphA4 kinase domain in the presence of [γ-^{32}P]ATP and either wild-type ephexin1 or a mutant form of ephexin1 in which Tyr87 was mutated to phenylalanine (ephexin1-Y87F). Under these conditions, wild-type ephexin1 was efficiently phosphorylated by both Src and the EphA4 kinase domain, but not by trkB (Figure 4C; Figure S3). Mutation of Tyr87 to phenylalanine abolishes ephexin1's ability to be phosphorylated by EphA4 and Src. Although these results suggest that Tyr87 is the site of EphA4/Src phosphorylation on ephexin1, it remained possible that mutation of Tyr87 to phenylalanine interferes with the phosphorylation of ephexin1 on a neighboring amino acid. Therefore, we used direct sequencing methods to identify which residue on ephexin1 becomes phosphorylated following in vitro incubation with Src. To this end, ephexin1 was phosphorylated in the presence of [γ-^{32}P]ATP and Src in vitro, and the tryptic peptide carrying the radioactive phosphate group was isolated by HPLC. Analysis of this tryptic peptide by Edman degradation confirmed that Tyr87 is the site of phosphorylation on ephexin1 (Figure 4D).

Since several commercially available anti-phosphotyrosine antibodies failed to detect the phosphorylation of Tyr87 on ephexin1, we generated an anti-ephexin1 phospho-Tyr87-specific antibody to monitor the phosphorylation status of Tyr87 of ephexin1 within cells. To test the specificity of the anti-ephexin1 phospho-Tyr87 antibody, we compared the antibody's affinity for phosphorylated and nonphosphorylated ephexin1 peptides that encompass amino acids 81 to 93 of ephexin1. We found that the anti-ephexin1 phospho-Tyr87 antibody binds effectively to phospho-ephexin1 peptide, but not to nonphosphorylated peptide (Figure 5A). To assess whether the anti-ephexin1 phospho-Tyr87 antibody selectively recognizes Tyr87 phosphorylation in the context of full-length ephexin, we incubated wild-type ephexin1 or ephexin1-Y87F with ATP and recombinant

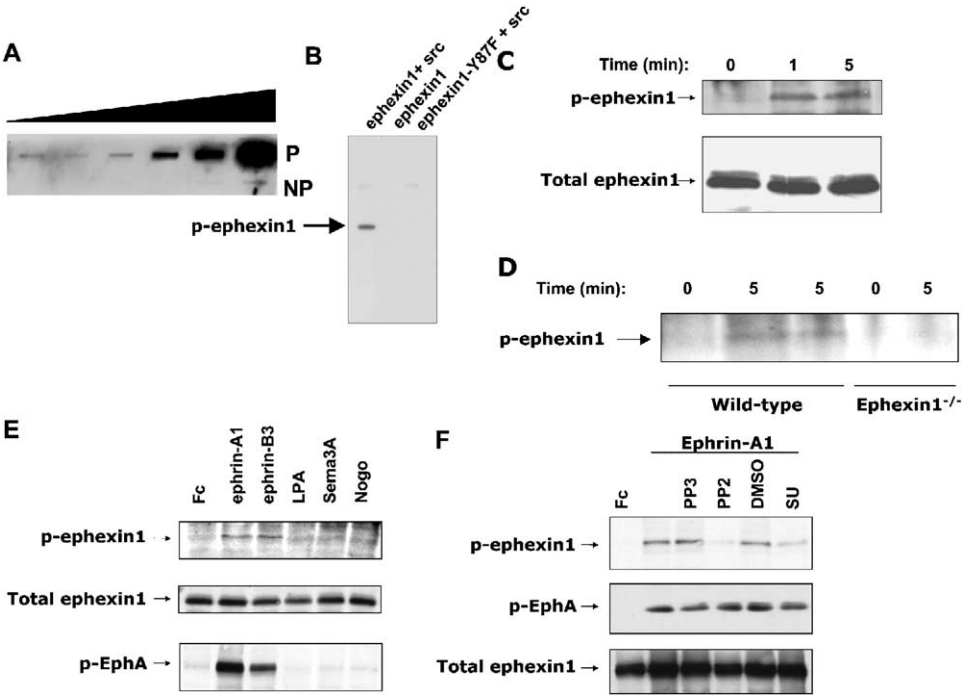

Figure 5. Characterization of the Anti-Ephexin1 Phospho-Tyrosine 87-Specific Antibody

(A) Slot blot analysis of phosphorylated (P) and nonphosphorylated (NP) peptides using the anti-ephexin1 phospho-tyrosine 87-specific antibody. Each slot represents a 10-fold higher concentration of peptide over the one to its left.

(B) Western blots of recombinant ephexin1 phosphorylated in vitro by Src, using anti-ephexin1 phospho-tyrosine 87-specific antibody. Immunoreactivity is detected with Src and ephexin1, but not ephexin1 alone or ephexin1-Y87F and Src, demonstrating the specificity of the anti-ephexin1 phospho-tyrosine 87 antibody.

(C) Ephexin1 is phosphorylated in neurons in response to ephrin treatment. Primary rat striatal neurons were cultured for 4 days and stimulated for the indicated amount of time with ephrin-A1. Lysates were probed with anti-ephexin1 phospho-tyrosine 87-specific (top panel) and total ephexin1 (bottom panel) antibodies. Ephexin1 tyrosine phosphorylation can be detected as early as 1 min after stimulation.

(D) Cultured primary striatal neurons from wild-type and *ephexin1*$^{-/-}$ mice were stimulated for the indicated amount of time with ephrin-A1. Lysates were probed with anti-ephexin1 phospho-tyrosine 87-specific antibody. Ephexin1 phosphorylation can be detected in wild-type neurons but not in *ephexin1*$^{-/-}$ neurons.

(E) Ephexin1 is phosphorylated specifically by ephrins. Primary rat striatal neurons were cultured for 4 days and stimulated with the indicated agents. Lysates were probed with anti-ephexin1 phospho-tyrosine 87-specific antibody, total ephexin1, and phospho-EphA antibodies.

(F) Inhibitors of Src family kinases block ephexin1 phosphorylation on Tyr87 without blocking activation of the Eph tyrosine kinases. Primary rat striatal neurons were cultured for 4 days and stimulated with Fc alone (first lane) or with ephrin-A1-Fc in the presence of no inhibitor (second lane), PP3, PP2, DMSO, or SU6656 (SU). Western blots were probed with anti-ephexin1 phospho-tyrosine 87-specific antibody, phospho-EphA, and total ephexin1 antibodies.

Src and examined the anti-ephexin1 phospho-Tyr87 antibody's binding to ephexin1 by Western blotting. We found that the anti-ephexin1 phospho-Tyr87 antibody specifically detects Tyr87 phosphorylated ephexin1, but not the ephexin1-Y87F mutant or nonphosphorylated wild-type ephexin1 (Figure 5B).

Ephrin Stimulation Results in Rapid Tyrosine Phosphorylation of Ephexin1 in Neurons

Given the importance of ephexin1 for ephrin-A-induced growth cone collapse in cultured neurons, we utilized the anti-ephexin1 phospho-Tyr87 antibody to determine whether ephexin1 is phosphorylated in response to EphA signaling in primary neuronal cultures. The anti-ephexin1 phospho-Tyr87 antibody recognized a protein of the appropriate molecular weight (75 kDa) in ephrin-A1-treated neurons (Figure 5C). To confirm that this protein is ephexin1, we compared lysates from wild-type and *ephexin1*$^{-/-}$ neurons. Importantly, no 75 kDa band is seen in the neuronal lysates from *ephexin1*$^{-/-}$ mice, even though Ephs are activated to the same extent as in wild-type neurons (Figure 5D; data not shown), suggesting that the 75 kDa band recognized by the anti-ephexin1 phospho-Tyr87 antibody upon ephrin-A treatment is the Tyr87 phosphorylated form of ephexin1. Using this antibody, we found that ephrin-A1 stimulation induces the phosphorylation of Tyr87 on ephexin1 in cultured neurons within 1 min (Figure 5C). Ephexin1 phosphorylation peaks at 5 min and begins to diminish by 30 min (Figure 5C; data not shown), paralleling the time course of growth cone collapse and reextension in these cultures. To determine whether ephexin1 Tyr87 phosphorylation can be induced by extracellular stimuli in addition to ephrin-A, we characterized the phosphorylation of ephexin1 on Tyr87 after exposure of neurons to several other extracellular factors. Ephrin-A1 and ephrin-B3 stimulation induced ephexin1 phosphorylation, while LPA, Sema-3a,

and Nogo did not induce the phosphorylation of this site, despite the ability of these agents to induce growth cone collapse (Figure 5E). Furthermore, other stimuli, such as BDNF, EGF, PDGF, and forskolin, did not result in the phosphorylation of ephexin1 on Tyr87 (data not shown). These observations demonstrate that ephexin1 Tyr87 phosphorylation occurs specifically in response to ephrin stimulation and correlates with the onset of ephrin-induced growth cone collapse, suggesting a specific role for this phosphorylation event in the process of Eph-dependent growth cone navigation.

Ephexin1 Is Phosphorylated in Neurons by Src Family Kinases

In vitro, both recombinant Src and the EphA4 kinase domain are able to phosphorylate ephexin1. To assess the importance of Src activation for ephrin-A1-induced ephexin1 phosphorylation in vivo, we took advantage of two small molecule inhibitors of the Src family of tyrosine kinases, PP2 and SU6656. Both PP2 and SU6656, but not PP3, the inactive analog of PP2, inhibited ephrin-A1-induced ephexin1 Tyr87 phosphorylation in cultured rat striatal neurons (Figure 5F). To ensure that, at the concentrations used, the pharmacological inhibitors were not inhibiting Eph tyrosine kinases, we titrated the concentration of the inhibitors to a level that did not affect ephrin-induced Eph phosphorylation in cultured neurons. We found that PP2 at 0.5 μM and SU6656 at 1 μM were specifically able to inhibit ephexin1 phosphorylation on Tyr87 but did not inhibit Eph tyrosine phosphorylation (Figure 5F). These findings suggest that ephrin-A1 binding to EphA leads to phosphorylation of ephexin1 at Tyr87 by activating Src family kinases. Consistent with our findings, Drescher and colleagues have recently reported that Src family kinases can phosphorylate ephexin1 in cultured neurons in response to ephrins (Knoll and Drescher, 2004).

Tyrosine Phosphorylation of Ephexin1 Contributes to Growth Cone Collapse

To determine whether phosphorylation of ephexin1 at Tyr87 is required for ephrin/Eph-dependent growth cone collapse, we transfected RGCs with wild-type and nonphosphorylatable forms (Y87F) of ephexin1 and analyzed the effect of these GEFs on ephrin-induced growth cone collapse. We have previously shown that ectopic expression of ephexin1 significantly potentiates ephrin-mediated growth cone collapse and that the GEF activity of ephexin1 is necessary for this effect (Shamah et al., 2001). While expression of wild-type ephexin1 or ephexin1-Y87F did not significantly alter the percentage of collapsed growth cones in unstimulated RGCs, RGCs expressing wild-type ephexin1 exhibited an increased percentage of collapsed growth cones in response to ephrin-A1 as compared to RGCs expressing vector alone (Figure 6A). In contrast, ephrin stimulation of RGCs expressing ephexin1-Y87F resulted in no increase in the percentage of growth cones that collapse when compared to RGCs expressing vector alone (Figure 6A). To determine whether an independent way of phosphorylating ephexin1 was sufficient to induce growth cone collapse, we sought to identify conditions under which ephexin1 was phosphorylated independently of ephrin stimulation. Since no other agent that we tested was able to induce the phosphorylation of Tyr87 on ephexin1, we sought to induce the phosphorylation of ephexin1 in neurons by blocking cellular tyrosine phosphatases. We found that pervanadate treatment of cultured neurons induced the phosphorylation of ephexin1 on Tyr87 and resulted in strong growth cone collapse response (Figure 6A; data not shown). Furthermore, pervanadate-treated RGCs expressing wild-type ephexin1 exhibited an increased frequency of growth cone collapse as compared to those expressing ephexin1-Y87F or vector alone, suggesting that pervanadate-induced phosphorylation of ephexin1 can also stimulate growth cone collapse (Figure 6A).

To the limit of our detection, we see no difference in subcellular localization or level of expression of wild-type ephexin1 and ephexin1-Y87F in RGCs (data not shown). Furthermore, both wild-type ephexin1 and ephexin1-Y87F bind EphA4 to a similar degree (Figure 6B). Thus, the observed difference in growth cone collapse between wild-type ephexin1 and ephexin1-Y87F was not a result of the mutant's aberrant localization or inability to bind Eph. Taken together, these data suggest that phosphorylation of ephexin1 at Tyr87 contributes to Eph-mediated growth cone collapse.

RGCs expressing ephexin1-Y87F did not show decreased growth cone collapse compared to RGCs expressing vector alone in response to either ephrin or pervanadate treatment. These data suggest that under the conditions of these experiments ectopically expressed ephexin1-Y87F may not interfere with the function of endogenous ephexin1. This may be because the endogenous ephexin1 is found in a stable complex with Ephs within cells and is not turned over within the time frame of the growth cone collapse experiments (24 hr). Alternatively, we may not be expressing ephexin1-Y87F at high enough levels to interfere with the function of the endogenous ephexin1.

Tyrosine Phosphorylation of Ephexin1 Mediates Cell Positioning in a Chick Spinal Cord

We next examined the role of ephexin1 tyrosine phosphorylation in vivo in the context of neural development using the chick embryo. To assess whether ephrin-A/EphA induction of ephexin tyrosine phosphorylation might be important for the proper development of LMC and/or MMC(m) neurons, we examined the effect of ectopic expression of either wild-type or a nonphosphorylatable mutant form of c-ephexin (c-ephexinY17F) on the behavior of motor neurons within the neural tube. It was difficult to examine the effect of ephexin on axon outgrowth and guidance because neurons ectopically expressing c-ephexin and EphA4 appear round and do not extend axons. Therefore, we concentrated our analysis on the migration and localization of motor neurons within the neural tube. Wild-type or Y17F mutant c-ephexin together with EphA4/EGFP were expressed in presumptive motor neurons in the ventral quadrant of the neural tube, as previously described (Eberhart et al., 2002; Krull, 2004). In control embryos, EGFP expression marks elongated neuroepithelial cells in the neural tube (Figure 7A). Ectopic expression of EphA4, wild-type c-ephexin, or c-ephexin-Y17F in the ventral neural

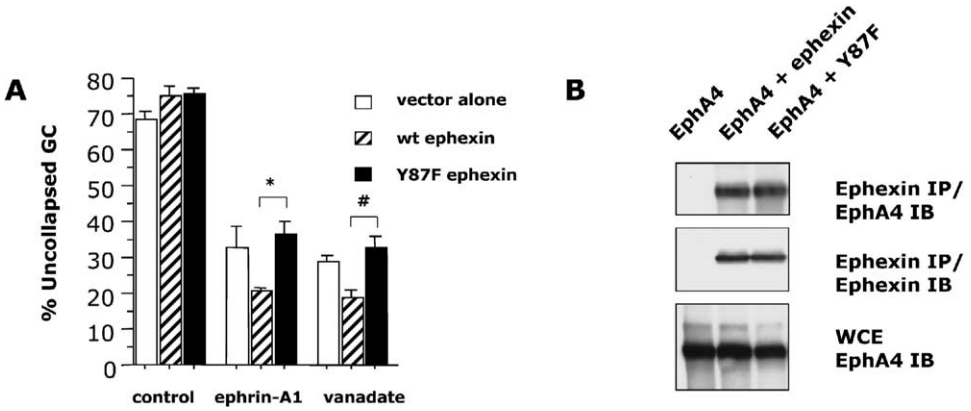

Figure 6. Ephexin1-Y87F Does Not Promote Ephrin-Mediated Growth Cone Collapse

(A) Purified RGCs were transfected with either vector alone (white bars), wild-type ephexin1 (hatched bars), or ephexin1-Y87F (black bars). Growth cone collapse was scored in a blinded manner for control, ephrin-A1-treated, and pervanadate-treated neurons. The data represent three separate experiments in which at least 100 growth cones were scored. All error bars are SEM; *$p < 0.001$; $p < 0.002$.

(B) Ephexin1-Y87F interacts with EphA4. The indicated constructs were transfected into HEK293T cells, and anti-ephexin1 immunoprecipitations were performed. Blots were probed with anti-EphA4 and anti-ephexin1 antibodies.

tube does not alter the positioning of motor neurons (data not shown; Eberhart et al., 2002). However, when EphA4/EGFP was expressed together with wild-type c-ephexin, many transfected neural tube cells prematurely exited the neural tube laterally, 24 hr after transfection (Figures 7B, 7C, and 7D). This aberrant migration was dependent on c-ephexin phosphorylation, as cells expressing EphA4/EGFP together with the c-ephexin-Y17F mutant did not migrate laterally but remained adjacent to the lumenal surface of the neural tube (Figures 7B, 7E, and 7F). Thus, ephrin-A/EphA induction of c-ephexin tyrosine phosphorylation can affect the localization of motor neurons and possibly other neural tube cells. Taken together with the observation that endogenous c-ephexin is restricted to LMC neurons in the developing spinal cord and our shRNA findings, these results suggest that EphA signaling through c-ephexin contributes to the proper localization of motor neurons in the ventral neural tube and to the targeting of their axons during spinal cord development.

Eph Modulation of Ephexin1 GEF Activity Requires Tyrosine Phosphorylation

Having found that ephexin1 tyrosine phosphorylation contributes to ephexin1 function in axon guidance and neuronal localization, we investigated the mechanism by which ephexin1 phosphorylation alters ephexin1 activity. To this end, we first determined which domains of ephexin1 confer specificity for the different Rho family GTPases. Upon expression of the catalytic domain of ephexin1, which is composed of the DH and PH domains, transfected REF-52 cells exhibit a predominantly RhoA-like phenotype, similar to that observed following activation of wild-type ephexin1 by EphA signaling (Figure 8A). As full-length ephexin1 activates RhoA, Rac1, and Cdc42, these results demonstrate that domains outside of the DH-PH domain confer substrate specificity on ephexin1. Furthermore, coexpression of EphA4 with ephexin1-DH-PH does not significantly affect the GEF activity of the catalytic domain, suggesting that additional ephexin1 domains are required to confer responsiveness to EphA signaling.

To determine which domains confer specificity on ephexin1, we generated a C-terminal truncation mutant of ephexin1 containing amino acids 1–518 only (ephexin1ΔC). This construct was able to induce RhoA, Rac1, and Cdc42 in REF-52 cells, and coexpression of EphA4 and ephexin1ΔC results in cells that exhibit a predominantly RhoA phenotype (data not shown). As the C terminus is not required to confer substrate specificity on ephexin1, we generated an N-terminal truncation mutant of ephexin1 (ephexin1ΔN) lacking amino acids 1–183 including the site of ephexin1 tyrosine phosphorylation. Cells expressing ephexin1ΔN exhibit a predominantly RhoA-like phenotype, mimicking the effect of the isolated ephexin1 catalytic domain (Figure 8A). Coexpression of EphA4 with ephexin1ΔN had no effect on the percentage of cells displaying a RhoA, Rac1, or Cdc42 phenotype when compared to cells expressing ephexin1ΔN alone. These results suggest that the N-terminal domain of ephexin1 acts to regulate ephexin1 GEF activity toward RhoA, Rac1, and Cdc42 and that phosphorylation of ephexin1 on Tyr87 in response to EphA activation might change ephexin1's substrate preference toward the three GTPases.

To test this hypothesis, we used the fibroblast morphology assay to assess the effect of wild-type ephexin1 and ephexin1-Y87F on RhoA, Rac1, and Cdc42 activity. When wild-type ephexin1 and ephexin1-Y87F were expressed in REF-52 fibroblasts, they were equally effective at activating RhoA (Figure 8B). Coexpression of EphA4 with wild-type ephexin1 led to an increase in the percentage of cells that exhibit a RhoA-like phenotype, while the percentage of cells displaying Rac1 and, to a lesser extent, Cdc42 phenotypes was diminished. In contrast, the coexpression of EphA4 with the nonphosphorylatable ephexin1 mutant (Y87F) had no effect on ephexin1-Y87F GEF activity toward RhoA (Figure 8B). Taken together, these data show that the N termi-

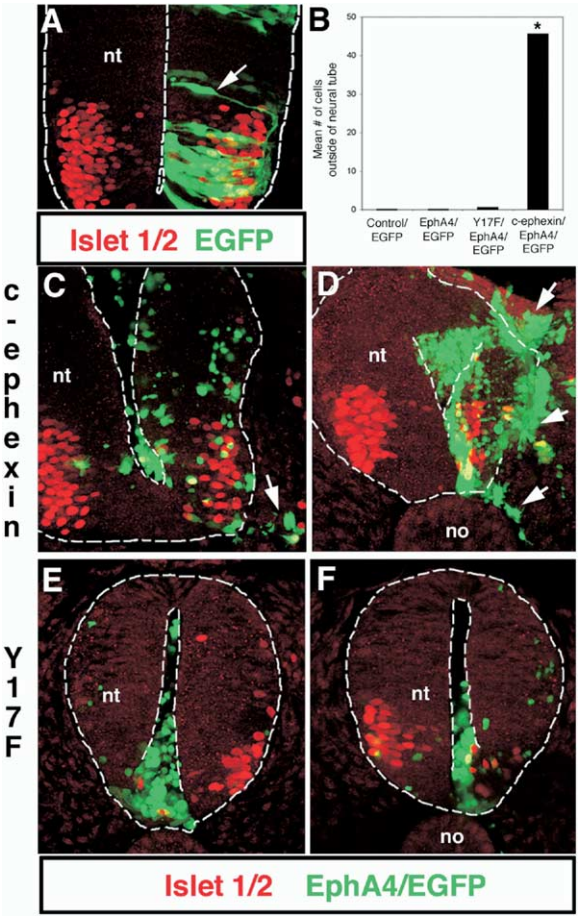

Figure 7. Phosphorylation of Ephexin1 Modulates Spinal Motor Neuron Localization

(A) Twenty-four hours after electroporation, neuroepithelial cells expressing EGFP (green) in control embryos demonstrate an elongated morphology, extending processes from the lumenal to pial surface (arrow). Islet-1/2-positive neurons are shown in red.

(B) Quantification of the mean number of cells outside the neural tube when c-ephexin or c-ephexinY17F is coexpressed with EphA4. Five embryos were analyzed for each condition. *p < 0.001.

(C and D) After 24 hr, cells coexpressing c-ephexin1/EGFP and EphA4/EGFP typically migrate aberrantly beyond the neural tube (arrows) and are often found misplaced in lateral positions.

(E and F) In the presence of c-ephexin1Y17F/EGFP and EphA4/EGFP, labeled cells do not migrate laterally but are found adjacent to the lumenal surface of the neural tube.

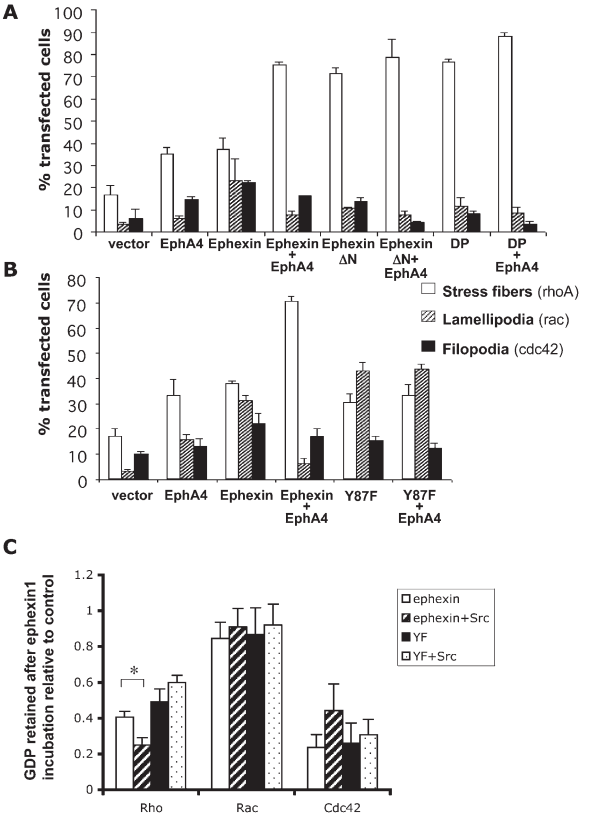

Figure 8. Phosphorylation of Ephexin1 Modulates Its GEF Activity toward Different GTPases

(A and B) REF-52 cells were transfected with the indicated constructs. Cells were stained with fluorescent phalloidin and scored for the presence of stress fibers (white bars), lamellipodia (hatched bars), and filopodia (black bars). All transfections were repeated six times, and at least 100 cells were scored for each experiment. Cells were scored in a blinded manner. All error bars are SEM.

(C) In vitro GDP release assay with recombinant proteins. Ephexin1 and ephexin1-Y87F were incubated with Src or GST prior to conducting the GDP release assay. GDP release was performed on RhoA, Rac1, and Cdc42. Data represent three individual experiments, and all error bars are SEM (*p < 0.002 by ANOVA).

nus of ephexin1 regulates its GEF activity and that the phosphorylation of ephexin1 on Tyr87 increases ephexin1's GEF activity toward RhoA relative to Rac1 and Cdc42. However, the experiments in REF-52 cells reflect the balance of all GTPases activated in the cell and thus do not distinguish between the following possibilities: (1) phosphorylation of ephexin1 could increase ephexin1's GEF activity toward RhoA and not change its activity toward Rac1 or Cdc42, (2) phosphorylation of ephexin1 could increase ephexin1's GEF activity toward RhoA while inhibiting its activity toward Rac1 or Cdc42, (3) phosphorylation of ephexin1 could suppress ephexin1's GEF activity toward Rac1 or Cdc42 and not change its activity toward RhoA. Any of these three possibilities could account for the observed REF-52 cell morphologies.

To distinguish between these possibilities, we directly assessed the effect of phosphorylation of Tyr87 on ephexin1's ability to catalyze the exchange of GDP for GTP on RhoA, Rac1, and Cdc42. We expressed recombinant ephexin1 and ephexin1-Y87F fused to GST from baculovirus-infected cells and tested the exchange activity of ephexin1 before and after in vitro phosphorylation by recombinant Src. In the in vitro GDP release assay, increased release of GDP from ephexin1 correlates with increased exchange activity. The exchange activity of wild-type ephexin1 toward RhoA was enhanced upon in vitro phosphorylation by Src, while the exchange activity of ephexin1 toward Rac1 and Cdc42 was not significantly altered by Src phosphorylation (Figure 8C). To assess whether the observed effect of Src on the exchange activity of ephexin1 is a result of phosphorylation, we tested the effect of Src

on the ability of ephexin1-Y87F to catalyze exchange of GTP for GDP on RhoA, Rac1, and Cdc42. We found that Src had no effect on the exchange activity of ephexin1-Y87F.

To ensure that what we observe in vitro accurately reflects what occurs in cells, we performed GDP release assays with lysates from transfected cells. We find that lysates from cells expressing ephexin1 and EphA4 exhibit higher exchange activity toward RhoA than lysates from cells expressing ephexin1 alone. This increase in exchange activity in the presence of EphA4 expression does not occur in lysates from cells expressing ephexin1-Y87F (data not shown). Thus, phosphorylation of ephexin1 at Tyr87 results specifically in an increase in ephexin1's GEF activity toward RhoA. Although this is the first example of a GEF changing its substrate preference in response to an extracellular stimulus, there are some recent examples of GAPs demonstrating such a switch. MgcRacGAP, which is a GAP for Rac/Cdc42, is converted to a RhoGAP upon phosphorylation by Aurora B kinase (Minoshima et al., 2003). Phosphorylation of mgcRacGAP by Aurora kinase increases the GAP activity of mgcRacGAP toward RhoA but not toward Rac1 or Cdc42.

We conclude that the phosphorylation of ephexin1 at Tyr87 within the N terminus of ephexin1 modulates ephexin1's GEF activity toward RhoA, Rac1, and Cdc42. However, rather than acting to generally suppress GEF activity, the ephexin1 N-terminal region regulates the substrate preference of ephexin1. Phosphorylation of ephexin1 on Tyr87 in response to ephrin-A/EphA signaling potentiates ephexin1-mediated activation of RhoA relative to Rac1 and Cdc42, thereby changing the local balance of Rho GTPase activity within cells. The switch in specificity may allow ephexin1 to promote axonal outgrowth in the absence of ephrin and growth cone repulsion when an Eph-expressing growth cone contacts ephrin-expressing cells. Consistent with this idea, *ephexin1*$^{-/-}$ neurons have reduced axonal outgrowth in the absence of ephrin and impaired growth cone collapse when treated with clustered ephrins.

Discussion

In the current study, we have tested the hypothesis that ephexin1 is required for ephrin-A-induced growth cone collapse and have elucidated a mechanism by which ephrin-A triggers ephexin1-dependent axon guidance. We find that chicken motor neurons in which ephexin protein has been knocked down by RNAi project prematurely into the hindlimb, indicating that ephexin plays a critical role in Eph-mediated axon guidance in vivo. In addition, we find that cultured RGCs from *ephexin1*$^{-/-}$ mice have significantly shorter axons, and their growth cones show reduced growth cone collapse in response to ephrin-A1 stimulation as compared with wild-type RGCs. These seemingly contrasting results—that ephexin1 is required for axonal outgrowth as well as for growth cone repulsion/collapse—are reconciled by our findings regarding the regulation of ephexin1 activity.

In the absence of ephrin, ephexin1 Tyr87 is not phosphorylated, and under these conditions, Eph bound ephexin1 activates RhoA, Rac1, and Cdc42, leading to a balance of GTPase activation that promotes axonal outgrowth. Consistent with this idea, RGCs that lack ephexin1 have shorter axons than wild-type RGCs. Ephexin1 could influence axonal outgrowth in one of two possible ways. Ephexin1 could be required either for the initiation of neurite development or for the promotion of axon outgrowth. As *ephexin1*$^{-/-}$ RGCs have a similar number of neurites when compared to wild-type RGCs, it is unlikely that the initiation of neurite outgrowth is regulated by ephexin. Furthermore, ephexin1 is tethered to the Eph at the plasma membrane of the growth cone, localizing ephexin1 to the proper place to regulate the rate of axonal extension.

While in the absence of ephrins ephexin1 promotes axonal outgrowth, ephrin stimulation of Ephs induces Src-dependent phosphorylation of ephexin1 on an evolutionarily conserved tyrosine, and this leads to growth cone collapse. The tyrosine phosphorylation of ephexin1 enhances ephexin1's exchange activity specifically toward RhoA, thus promoting growth cone collapse/repulsion. Consistent with this idea, we find that ephexin1 is important for ephrin-mediated growth cone collapse in vitro and axon guidance in vivo. Chicken motor neuron axons in which ephexin has been knocked down enter the hindlimb prematurely. Since motor neuron projections into the hindlimb have previously been shown to be controlled by ephrin/Eph interactions (Eberhart et al., 2002), this result strongly suggests that ephexin is required for Eph/ephrin-mediated axon guidance in vivo. This defect in axon guidance most likely reflects impairment in the ability of ephexin-deficient axonal growth cones to collapse in response to ephrins in limb mesoderm, as the growth cones of cultured RGCs from *ephexin1*$^{-/-}$ mice display a defective collapse response when exposed to ephrin.

In addition to demonstrating that ephexin1 plays a key role in ephrin-mediated collapse/repulsion, our findings identify a mechanism by which Ephs regulate ephexin1, leading to growth cone collapse. The directional control of axon pathfinding in vivo is thought to result from local modulation of the actin cytoskeleton such that growth cones turn away from repellents and toward attractants. The discoveries that ephexin1 is required for axon outgrowth, is regulated by tyrosine phosphorylation, and when tyrosine phosphorylated promotes growth cone collapse suggest a mechanism by which Rho GTPases could control the actin cytoskeleton in the highly localized manner that is required for accurate growth cone guidance. Since ephexin1 is constitutively bound to Ephs, its effects on Rho GTPases may remain confined to the vicinity of the Eph complex. Thus, in the absence of ephrin stimulation, Eph/ephexin1 complexes might promote localized growth cone extension. When Ephs are activated in a portion of the growth cone by ephrins, local tyrosine phosphorylation of ephexin1 at Tyr87 could tip the local balance of GTPase activity toward RhoA, leading to actin cytoskeletal changes that result in local retraction. In regions of the growth cone that have not made specific contact with ephrin, ephexin1 might still promote growth by activating RhoA, Rac1, and Cdc42. This could result in directed movement of the growth cone

away from ephrin-expressing zones and toward its ultimate target.

If ephexin1 bound to Ephs is to play the dual role of promoting outgrowth in the absence of ephrins and retraction in the presence of ephrins, one might predict that ephexin1 may have evolved to specifically interact with Ephs and not other guidance receptors. For example, if ephexin1 interacted with Ephs and plexins (a receptor for the repulsive guidance factor semaphorin) at the same time and in the same region of the growth cone, conflicting signals might occur depending on the presence of ephrins and semaphorins. If ephrin were present and semaphorin were not, ephexin1 bound to Ephs could signal the growth cone to retract, while ephexin1 bound to plexins would signal the growth cone to extend. To avoid this problem, ephexins appear to have evolved so that they specifically mediate ephrin/Eph signaling. Consistent with this idea, we find that, of the growth and guidance factors tested, only ephrin is able to induce ephexin1 phosphorylation on Tyr87. No other guidance molecules (e.g., BDNF, LPA, Sema3A, or Nogo66) or growth factors (e.g., PDGF, EGF, or insulin) tested led to ephexin1 tyrosine phosphorylation, suggesting that ephexin1 may be specifically designed to respond to ephrin signals. Since ephexin1 can promote outgrowth in the absence of ephrin and repulsion upon encountering ephrins, ephexin1 is tailored to mediate ephrin-dependent growth cone guidance.

To better understand the process by which Ephs mediate axon guidance, we investigated how tyrosine phosphorylation of ephexin1 switches ephexin1's exchange activity. Through mutagenesis of ephexin1, we found that the isolated DH/PH domain possesses strong exchange activity toward RhoA and is ineffective at activating Rac1 and Cdc42. In the context of full-length ephexin1 when Tyr87 is not phosphorylated, the DH/PH domain is capable of activating RhoA, Rac1, and Cdc42. This suggests that, in the absence of phosphorylation, other domains of ephexin1 modulate the activity of the DH/PH domain so that it no longer preferentially activates RhoA. Further mutagenesis revealed that it is the N terminus that possesses the modulatory function. Tyr87 phosphorylation in response to ephrin appears to suppress the modulatory effect of the N terminus, resulting in an ephexin1 DH/PH domain that is highly selective toward RhoA at the expense of Rac1 and Cdc42. Consistent with such a model, we find that full-length ephexin1 when not phosphorylated in vitro is capable of activating RhoA, Rac1, and Cdc42. When phosphorylated at Tyr87 in vitro, ephexin1's activity for RhoA is specifically enhanced, while its activity toward Rac1 and Cdc42 is unchanged. This suggests that within cells the phosphorylation of ephexin1 in response to Eph activation leads to a potentiation of RhoA activity and possibly enhances binding to RhoA so that ephexin1 is unavailable to activate Rac1 and Cdc42. Further experimentation will be required to assess binding affinities of nonphosphorylated and phosphorylated ephexin1 for RhoA relative to Rac1 and Cdc42. While it is presently not clear how tyrosine phosphorylation specifically suppresses the N-terminal modulatory effect on the DH/PH domain, one likely effect is that the N terminus interacts directly with the DH/PH domain to modulate DH/PH domain function. Consistent with this possibility, we find that the isolated N terminus of ephexin is capable of interacting with an isolated fragment of ephexin1 consisting of the DH/PH domain and the C terminus (data not shown).

While our experiments reveal that ephexin1 plays a significant role in Eph-mediated axon guidance, it remains to be determined whether ephexin1 plays a role in other Eph-dependent biological processes. One possibility is that ephexin1 may mediate Eph-dependent effects on cell migration and localization. Consistent with this possibility, we have found that overexpression of chicken ephexin leads to aberrant migration of presumptive motor neurons out of the neural tube, a process that is dependent on the phosphorylation of ephexin. In addition to migration, Ephs have also been implicated in dendritic spine formation. Similar to growth cones, dendritic spines are highly motile actin-based structures that rapidly alter their morphology in response to various extracellular stimuli (including ephrins). Thus, ephexin family GEFs may mediate some aspects of ephrin-dependent dendritic spine formation and/or maintenance. In this regard, our preliminary results suggest that ephexin5 is highly enriched in dendritic spines and thus might play an important role in regulating dendritic spine formation.

While ephexin1 appears capable of modulating actin cytoskeletal dynamics during growth cone guidance, remodeling of the cytoskeleton is not the only cellular process that is required for regulation of axon guidance. The process of axon guidance is a complex event involving endocytosis of plasma membrane and cell surface proteins, reorganization of the actin cytoskeleton and microtubules, and local protein translation and degradation (van Horck et al., 2004). The signaling pathways that link cell surface receptor activation to each of these processes are not yet well understood. While we have shown that ephexin1 regulates the balance of GTPase activation, thereby affecting the actin cytoskeleton during the process of axon guidance, it is not yet clear if ephexin1 is involved in other steps in the process of axon guidance such as endocytosis, local protein translation, and local protein degradation. We have recent evidence that another GEF, Vav2, is important for Eph-dependent axon guidance (Cowan et al., 2005 [this issue of *Neuron*]). In response to ephrin stimulation, Vav2 associates with the Ephs, becomes tyrosine phosphorylated, and plays a role in ephrin/Eph-dependent endocytosis that is a key step in Eph-dependent axon guidance. It remains to be determined whether or not ephexin and Vav function independently of each other and how these two GEFs and other proteins that interact with Ephs coordinate the complex process of axon guidance.

Experimental Procedures

In Vitro Kinase Assays

Recombinant ephexin was incubated with either GST-EphA4 kinase domain or His-tagged Src (Upstate Biotechnology) in kinase buffer (20 mM Tris 7.5, 8 mM $MgCl_2$, 3 mM $MnCl_2$) with 200 μM ATP and 5 μCi [γ-^{32}P]ATP for 30 min at 30°C. For trkB kinase assays, Flag-tagged trkB was transfected into HEK293T cells and immunoprecipitated with anti-Flag epitope antibody before incubating with

ephexin1 in kinase buffer. Samples were electrophoresed on an SDS-PAGE gel that was subsequently stained with Coomassie blue and exposed to film.

Fibroblast Morphology Assay

REF-52 cells were maintained in DMEM with 10% newborn calf serum, glutamine, and Pen/Strep (Invitrogen) and transfected using Fugene (Roche). Twenty-four to forty-eight hours after transfection, cells were fixed with 4% paraformaldehyde, permeabilized with 0.1% Triton, and stained with Alexa594-conjugated phalloidin (Molecular Probes). Cells were scored in a blinded manner.

Growth Cone Collapse Assay and Axon Length Analysis

RGCs were purified and cultured as previously described (Meyer-Franke et al., 1995). Expression plasmids were electroporated into RGCs with the rat neuron Nucleofector kit (Amaxa). RGCs that were cultured for 1–2 days were stimulated with aggregated ephrins for 30 min, fixed in 4% paraformaldehyde, stained with Alexa594-conjugated phalloidin (Molecular Probes), and scored for growth cone collapse in a blinded manner. Ephrin-A1-Fc was aggregated at 5 μg/ml 45 min prior to use with 0.45 mg/ml goat anti-human Fc antibody (Jackson Laboratories) in Dulbecco's phosphate-buffered saline (Invitrogen). Pervanadate was prepared as previously described (Sun et al., 2000), and RGCs were treated with 10 μM pervanadate for 30 min.

For neurite length analysis of dissociated neurons, neurons were fixed after 24–36 hr in culture and stained with phalloidin-Texas red (Molecular Probes). Images blinded to the experimenter were obtained on a fluorescent microscope and were analyzed using Metamorph software (Universal Imaging Corporation) by manually tracing the length of the neurite for at least 50 neurons per condition. Four independent experiments were conducted for each mouse strain.

RNA Interference

The full-length chicken ephexin sequence was copied into the siRNA search engine (http://jura.wi.mit.edu/siRNAext/). Two oligo sequences against chicken ephexin were generated: 218 and 461. These regions were not homologous to any other known genes, as determined by BLAST search. Each sequence was then entered into a siRNA converter (http://www.ambion.com/techlib/misc/psilencer_converter.html/), to generate top and bottom oligo sequences that were acquired (Sigma-Genosys). C-ephexin 461 top sequence, 5′-GGCTGTTAGTGAGCGCTTCTTCAAGAGAGAAGCGCTCACTAACAGCCTTTTTT-3′; c-ephexin 461 bottom sequence, 5′-AATTAAAAAAGGCTGTTAGTGAGCTTCTCTCTTGAAGAAGCGCTCACTAACAGCCGGCC-3′; c-ephexin 218 top sequence, 5′-GCTCCAACTCCAGGTTCAACTTCAAGAGAGTTGAACCTGGAGTTGGAGTTTTTT-3′; c-ephexin 218 bottom sequence, 5′-AATTAAAAAACTCCAACTCCAGGTTCAACTCTCTTGAAGTTGAACCTGGAGTTGGAGCGGCC-3′. Briefly, the complementary oligonucleotides were annealed and inserted into the ApaI/EcoRI sites of the pSilencer 1.0 U6 vector (Ambion). Missense shRNAs were generated by changing three bases in the c-ephexin 218 and 461 constructs. Mutated bases are underlined: 218 missense, 5′-CTGCAACTACAGGTTCACC-3′; 461 missense, 5′-GCCTGTTAGGGAGCGCTAC-3′. These missense sequences were then subjected to BLAST and BBSRC query; no similarities to chicken or mammalian sequences were identified. Missense oligos were annealed and placed in pSilencer 1.0 U6, as described above. All shRNAs were confirmed by sequence analysis.

Quantification of Ephexin Protein Levels

To quantify ephexin protein levels, the average pixel intensity of presumptive LMC neurons in unsaturated single optical sections acquired by confocal microscopy was determined using Fluoview software (Olympus). Sections acquired from three different treatment conditions were measured: (1) ephexin shRNA-expressing; (2) missense shRNA-expressing; and (3) pCAX (EGFP)-expressing. Three readings were performed for each LMC domain on the transfected side and nontransfected side.

In Ovo Electroporation

Fertilized White Leghorn chicken eggs (Hy-Line International, Spencer, IA; Bilbie Aviaries, Ann Arbor, MI) were incubated at 38°C in a humidified incubator until stage 17 of development. For transfection, 2.0–2.5 μg/μl of shRNA was coelectroporated with pCAX/EGFP (2–2.5 μg/μl) into a ventral quadrant of the neural tube of stage 17 embryos, as previously described (Eberhart et al., 2002). For electroporations to express EGFP (2 μg/μl) or to coexpress c-ephexin/EGFP or c-ephexin-Y17F/EGFP with EphA4/EGFP, stage 15–17 chick embryos were coelectroporated with 2–2.5 μg/μl of each construct. Five 14V (Protech Int., TX) or 19V–22V pulses (BTX/Genetronics, CA) of 50 ms duration were applied, and several drops of Ringer's buffer were added, after which each egg was sealed with tape and incubated for 6, 12, 24, or 32 hr.

GDP Release Assays

In vitro guanine nucleotide release assays were performed as described elsewhere (Debant et al., 1996) using recombinant full-length ephexin1 with RhoA-His, Rac1-His, and Cdc42-His (Cytoskeleton). Briefly, the GTPases were first loaded with ^{3}H-GDP in exchange buffer (50 mM Tris [pH 7.5], 50 mM NaCl, 5 mM EDTA, 1 mM DTT, 1 mg/ml BSA). After incubation, $MgCl_2$ was added to a final concentration of 5 mM, and proteins were maintained on ice. Recombinant ephexin1 was incubated with the GTPase in 50 mM Tris (pH 7.5), 1 mM GTP, 2 mM $MgCl_2$ at room temperature for 15 min. In the presentation of data, the intrinsic GDP release rate of the GTPase is taken into account. Thus, "100%" corresponds to the amount of protein bound ^{3}H-GDP retained on the filter in the presence of the GTPase alone.

Supplemental Data

The Supplemental Data include three supplemental figures and Supplemental Experimental Procedures and can be found with this article online at http://www.neuron.org/cgi/content/full/46/2/191/DC1/.

Acknowledgments

The authors thank Margaret Thompson, Yiping Zhou, and Hong Ye for assistance in generating *ephexin1*$^{-/-}$ mice; Pieter Dikkes for assistance with immunohistochemistry and in situ hybridization experiments; Sara Vasquez for assistance with neuronal cell cultures; David L. Brautigan for providing REF-52 cells; Rudiger Klein and Joaquim Egea for sharing unpublished results; and Eric Griffith, Janine Zieg, Ben Barres, Mitsuhiro Makino, Beth Perkins, and members of the Greenberg lab for critical discussions. M.E.G. acknowledges the generous support of the F.M. Kirby Foundation to the Children's Hospital Neurobiology Program. This work was supported by National Institute of Child Health and Human Development grant K08 HD01384 (M.S.); the William Randolph Hearst Fund (M.S.); a National Defense Science and Engineering graduate fellowship (M.Z.L.); a National Science Foundation predoctoral fellowship (P.L.G.); a Muscular Dystrophy Association postdoctoral fellowship (S.O.); National Institute of Mental Health grant R01 MH59894 (C.E.K.); National Institute of Neurological Disorders and Stroke grant R01 NS35884 (G.C.); Mental Retardation Research Center grant HD18655 and National Institutes of Health grant NS45500 (M.E.G.); and a grant from Daiichi Pharmaceuticals (M.E.G.).

Received: July 9, 2004
Revised: December 3, 2004
Accepted: January 18, 2005
Published: April 20, 2005

References

Cowan, C.W., Shao, Y.R., Sahin, M., Shamah, S.M., Lin, M.Z., Greer, P.L., Gao, S., Griffith, E.C., Brugge, J.S., and Greenberg, M.E. (2005). Vav family GEFs link activated Ephs to endocytosis and axon guidance. Neuron *46*, 205–217.

Debant, A., Serra-Pages, C., Seipel, K., O'Brien, S., Tang, M., Park, S.H., and Streuli, M. (1996). The multidomain protein Trio binds the LAR transmembrane tyrosine phosphatase, contains a protein kinase domain, and has separate rac-specific and rho-specific guanine nucleotide exchange factor domains. Proc. Natl. Acad. Sci. USA *93*, 5466–5471.

Dickson, B.J. (2002). Molecular mechanisms of axon guidance. Science *298*, 1959–1964.

Eberhart, J., Swartz, M.E., Koblar, S.A., Pasquale, E.B., and Krull, C.E. (2002). EphA4 constitutes a population-specific guidance cue for motor neurons. Dev. Biol. *247*, 89–101.

Eberhart, J., Barr, J., O'Connell, S., Flagg, A., Swartz, M.E., Cramer, K.S., Tosney, K.W., Pasquale, E.B., and Krull, C.E. (2004). Ephrin-A5 exerts positive or inhibitory effects on distinct subsets of EphA4-positive motor neurons. J. Neurosci. *24*, 1070–1078.

Feldheim, D.A., Vanderhaeghen, P., Hansen, M.J., Frisen, J., Lu, Q., Barbacid, M., and Flanagan, J.G. (1998). Topographic guidance labels in a sensory projection to the forebrain. Neuron *21*, 1303–1313.

Flanagan, J.G., and Vanderhaeghen, P. (1998). The ephrins and Eph receptors in neural development. Annu. Rev. Neurosci. *21*, 309–345.

Huber, A.B., Kolodkin, A.L., Ginty, D.D., and Cloutier, J.F. (2003). Signaling at the growth cone: ligand-receptor complexes and the control of axon growth and guidance. Annu. Rev. Neurosci. *26*, 509–563.

Jurney, W.M., Gallo, G., Letourneau, P.C., and McLoon, S.C. (2002). Rac1-Mediated Endocytosis during Ephrin-A2- and Semaphorin 3A-Induced Growth Cone Collapse. J. Neurosci. *22*, 6019–6028.

Knoll, B., and Drescher, U. (2004). Src family kinases are involved in EphA receptor-mediated retinal axon guidance. J. Neurosci. *24*, 6248–6257.

Krull, C.E. (2004). A primer on using in ovo electroporation to analyze gene function. Dev. Dyn. *229*, 433–439.

Meyer-Franke, A., Kaplan, M.R., Pfrieger, F.W., and Barres, B.A. (1995). Characterization of the signaling interactions that promote the survival and growth of developing retinal ganglion cells in culture. Neuron *15*, 805–819.

Minoshima, Y., Kawashima, T., Hirose, K., Tonozuka, Y., Kawajiri, A., Bao, Y.C., Deng, X., Tatsuka, M., Narumiya, S., May, W.S., et al. (2003). Phosphorylation by Aurora B Converts MgcRacGAP to a RhoGAP during Cytokinesis. Dev. Cell *4*, 549–560.

Moolenaar, W.H. (1999). Bioactive lysophospholipids and their G protein-coupled receptors. Exp. Cell Res. *253*, 230–238.

Nobes, C.D., and Hall, A. (1995). Rho, rac, and cdc42 GTPases regulate the assembly of multimolecular focal complexes associated with actin stress fibers, lamellipodia, and filopodia. Cell *81*, 53–62.

Ogita, H., Kunimoto, S., Kamioka, Y., Sawa, H., Masuda, M., and Mochizuki, N. (2003). EphA4-mediated Rho activation via Vsm-RhoGEF expressed specifically in vascular smooth muscle cells. Circ. Res. *93*, 23–31.

Palmer, A., and Klein, R. (2003). Multiple roles of ephrins in morphogenesis, neuronal networking, and brain function. Genes Dev. *17*, 1429–1450.

Penzes, P., Beeser, A., Chernoff, J., Schiller, M.R., Eipper, B.A., Mains, R.E., and Huganir, R.L. (2003). Rapid induction of dendritic spine morphogenesis by trans-synaptic ephrinB-EphB receptor activation of Rho-GEF kalirin. Neuron *37*, 263–274.

Shamah, S.M., Lin, M.Z., Goldberg, J.L., Estrach, S., Sahin, M., Hu, L., Bazalakova, M., Neve, R.L., Corfas, G., Debant, A., and Greenberg, M.E. (2001). EphA receptors regulate growth cone dynamics through the novel guanine nucleotide exchange factor ephexin. Cell *105*, 233–244.

Sun, Q.L., Wang, J., Bookman, R.J., and Bixby, J.L. (2000). Growth cone steering by receptor tyrosine phosphatase delta defines a distinct class of guidance cue. Mol. Cell. Neurosci. *16*, 686–695.

Van Aelst, L., and D'Souza-Schorey, C. (1997). Rho GTPases and signaling networks. Genes Dev. *11*, 2295–2322.

van Horck, F.P., Weinl, C., and Holt, C.E. (2004). Retinal axon guidance: novel mechanisms for steering. Curr. Opin. Neurobiol. *14*, 61–66.

Wahl, S., Barth, H., Ciossek, T., Aktories, K., and Mueller, B.K. (2000). Ephrin-A5 induces collapse of growth cones by activating rho and rho kinase. J. Cell Biol. *149*, 263–270.

Winning, R.S., Ward, E.K., Scales, J.B., and Walker, G.K. (2002). EphA4 catalytic activity causes inhibition of RhoA GTPase in Xenopus laevis embryos. Differentiation *70*, 46–55.